substance: boron compounds with group IV elements: boron carbide
property: optical properties

Calculated optical properties (optical conductivity σ, real and imaginary part of the dielectric function, and energy-loss function) of hypothetical $B_{13}C_2$ (Fig. 1) and $B_{11}C$(CBC) (Fig. 2) [95L].

dielectric function

ε_1 at 100 Hz

ε_1	31	T = 300 K	10 at. % C	93S
	59		15.4 at % C	
	22		18.1 at. % C	
	23		18.7 at. % C	

ε_1 at 10^{10} Hz

ε_1	7.5(8)	T = 300 K	10 at. % C	93S
	9.0(8)		13.1 at. % C	
	9.6(8)		15.4 at % C	
	20(8)		18.1 at. % C	
	25(8)		20 at. % C	

Temperature dependence of the real part of the dielectric function and tan δ for $B_{4.5}C$ and B_9C in Fig. 3 [93S].

Frequency dependence of the real part of the dielectric function ε_1 for B_xC (x = 4.33, 4.5, 5.5, 9.0) at 4 K in Fig. 4 [93S].

Frequency dependence of the real part of the dielectric function ε_1 for $B_{4.3}C$ (T =8,15, 22, 36, 46 and 60 K) and $B_{13}C_2$ (T =4, 10 and 40 K) in Fig. 5 [91Z, 91P, 91S1].

Temperature dependence of the dielectric function of B_4C at 9 GHz in Fig. 6 [91Z].

Real part of the dielectric function of $B_{4.3}C$ vs. frequency. Experimental results [98S1, 99S2, 91Z] compared with model calculations [98S1, 99S2] based on different theories (extended Drude model [85M], hopping model [73B], potential fluctuations [84P], random free energy barrier model [88D]) in Fig. 7.

FIR experimental spectra of the real part of the dielectric function and the optical conductivity of $B_{6.3}C$ (as an example) simultaneously fitted according to different transport models in Fig. 8 [98S1, 99S2].
Real and imaginary part of the dielectric function of boron carbides with different chemical compositions ($B_{4.23}C$, $B_{4.51}C$, $B_{6.28}C$, $B_{8.52}C$, $B_{10.37}C$) and $^{10}B_{4.3}C$ (92% isotope enriched) in Fig. 9 [97W].

Dielectric function in the optical range in [91S2, 93S].

absorption edge/interband transitions

Model calculation for the absorption coefficient of small polarons in [93E].

Absorption edge at 300 K in Fig. 10 [92W].

Temperature dependence of the absorption edge in Fig. 11 [92W].

Reflectance spectrum of boron carbide 1.8...5 eV in Fig. 12 [94H].

Structure-modulated reflectivity spectra and their first derivatives obtained on boron carbide with compositions close to the carbon-rich limit of the homogeneity range in Fig. 13 [96W].

Structure-modulated reflectivity spectra of $B_{4.01}C$, $B_{4.5}C$, $B_{6.2}C$, $B_{6.4}C$, $B_{6.9}C$, $B_{7.2}C$, $B_{8.5}C$, $B_{10.42}C$ related to $B_{4.23}C$ in Fig. 14 [96W].

Optical absorption of carbon-doped β-rhombohedral boron and boron carbide in the absorption edge range [91W2].

IR

FIR reflectivity spectra of $B_{4.3}C$, $B_{6.3}C$ and $B_{10.37}C$ for 90, 300 and 450 K in Fig. 15 [98S1, 99S2] (For spectra of $B_{7.91}C$ and $B_{8.52}C$ see reference).

Optical spectra of the IR active phonons of $B_{4.3}C$, $B_{6.3}C$, $B_{7.91}C$, $B_{8.52}C$ and $B_{10.37}C$ in Fig. 16 [92K2, 92K1, 94K1, 94K4].

Optical spectra of the IR active phonons of $B_{4.3}C$ for 30, 160, 300 and 450 K in Fig. 17 [92K2, 92K1, 94K1].

Optical phonon spectra of $B_{4.3}C$ depending on crystal orientation and isotope enrichment in Fig. 18 [92K2, 92K1, 94K1].

IR spectra of isotope-enriched boron carbide $^{10}B_{4.3}C$, $^{11}B_{4.3}C$, $^{10}B_{4.3}{}^{13}C$ in Fig. 19. For the corresponding spectra of $B_{6.5}C$ and $B_{10}C$ see reference [99W2]. For phonon frequencies see above (lattice properties)

Absorption spectra of the streching mode of the three-atom chain for different chemical compositions and isotope enrichments in Fig. 20 [92K2, 92K1, 94K1].

Powder IR phonon spectra [81B1].

IR spectra in [87W2].

IR phonon reflectivity spectrum compared with other icosahedral boron-rich solids in [87W1].

IR phonon spectra of boron carbide depending on the composition in [91W1].

Reflectivity spectra in the phonon range in [93S].

IR reflectivity and powder transmission spectra for different compositions and isotope enrichments; quenching of the 1055/1092 cm^{-1} phonon by illumination [93W].

IR phonon absorption spectra in [90W].

IR reflectance spectra and dielectric function of boron carbide with different composition in [91T3] (from the spectra it can be seen that the sample surfaces were covered with foreign absorbing substances).

Raman

For boron carbide (and some other icosahedral boron-rich compounds as well) the published Raman spectra are qualitatively different, when obtained by the conventional method using lasers with high photon energies (e.g. Ar-Laser with 2.41 eV) for excitation, which exceed the interband transition energy of boron carbide, or when obtained by FTIR Raman spectrometers using Nd:YAG lasers (1.16 eV) (see Fig. 21). By systematic investigations [99W1, 99W3] it was definitely excluded that the high intensity of Nd:YAG was responsible for this difference. A comparison with the Raman spectra of other boron compounds (in particular boron oxides) suggest that – because of the considerably smaller penetration depth at the higher photon energies – the conventionally measured Raman spectra are essentially determined by surface layers probably resulting from chemical reaction with the surrounding atmosphere. Therefore, below only FT-Raman spectra of boron carbide are reproduced. For the conventionally measured Raman spectra the references are given only.

Comparison of a FT-Raman spectrum of $B_{4.3}C$ [93K, 94K1, 94K2, 94K3] and a conventionally measured Raman spectrum of B_4C [88T, 89T, 91T1, 90A] in Fig. 21.

FT-Raman spectra of $^{10}B_{4.3}C$ and $^{nat}B_{4.3}C$ (unpolarized and polarized) in Fig. 22 [94K1].

FT Raman spectra of boron carbide of different chemical composition in Fig. 23 [94K1, 94K2, 94K3].

conventionally measured Raman spectra:

Raman investigations in [86S].

Raman spectra in [88T, 89T].

Isotope-dependent Raman spectra in [91T1].

Raman spectra in connection with preparation and properties of icosahedral borides [90A].

Raman spectra of pure and P-doped boron carbide in [93A, 94A].

Isotope dependencies of Raman spectra of $B_{12+x}C_{3-x}$ compared with $B_{12}As_2$, $B_{12}P_2$, $B_{12}O_2$ in [97A].

Further figures:

Absorption: Fig. 24, photo-absorption: Fig. 25, occupation of traps by photoexcitation: Fig. 26, reflectivity: Fig. 27, dependence of optical parameters on C content: Figs. 28...30.

For Auger investigations, see [77D].

References:

65L Lucovsky, G.: Solid State Commun. 3 (1965) 299.

71W Werheit, H., Binnenbruck, H., Hausen, A.: Phys. Status Solidi (b) 47 (1971) 153.

73B Butcher, P.N., Morys, P.L.: J. Phys. C 6 (1973) 2147.

74K Korsukova, M. M., Gurin, V. N., Sorokin, V. N., Yusov, Yu. P., Terent'eva, S. P., in: Bor, Poluchenie, Struktura i Svoistva, Ed.: Tavadze F. N., Moscow Nauka, 1974, p. 235.

74W Werheit, H., Binnenbruck, H.: see [74K], p. 110.

77D Dagourry, G., Vigner, D.: Le Vide 187 (1977) 51.

79B Binneabruck, H., Werheit, H.: Z. Naturforsch. 34a (1979) 787.

79W Werheit, H.: J. Less-Common Met. 67 (1979) 143.

81A Armstrong, D. R.: Proc. 7th Int. Symp. Boron, Borides and Related Compounds. Uppsala, Sweden, 1981; spec. issue of J. Less-Common Met. 82 (1981) 357.

81B1 Bouchacourt, M., Thevenot, F.: J. Less-Common Met. 82 (1981) 227 (Proc. 7th Int. Symp. Boron, Borides and Rel. Compounds, Uppsala, Sweden, 1981).

81B2 Bouchacourt, M., Thevenot, F.: see [81A], p. 227.

81E Ekbote, S.N., Narlikar, A.V.: Curr. Sci. 50 (1981) 674.

82W Werheit, H.: Colloque FranceAllemand Ceramiques Techniques Lyon, March 1517; 1983, Nr. 3-4-p.

84P Pistoulet, B., Roche, F.M., Abdalla, S.: Phys. Rev. B 30 (1984) 5987.

85M Mott, N.F., Kaveh, M.: Adv. Phys. 34 (1985) 329.

86S Shelnutt, J.A., Morosin, B., Emin, D., Mullendore, A., Slack, G.A., Wood, C.: in: Boron-Rich Solids (AIP Conf. Proc. 140), Albuquerque, New Mexico 1985, D. Emin, T.L. Aselage, C.L. Beckel, I.A. Howard ed., American Institute of Physics: New York, 1986, p. 312.

87W1 Werheit, H.: in: Proc. 9th Int. Symp. Boron, Borides and Rel. Compounds, University of Duisburg, Germany, Sept. 21 - 25, 1987, H. Werheit ed., University of Duisburg: Duisburg, 1987, p. 142.

87W2 Werheit, H., Haupt, H.: Z. Naturforsch. 42a (1987) 925.

88D Dyre, C.D.: J. Appl. Phys. 64 (1988) 2456.

88T Tallant, D.R., Aselage, T.L., Campbell, A.N., Emin, D.: J. Non-Cryst. Solids 106 (1988) 370.

89T Tallant, D.R., Aselage, T.L., Campbell, A.N., Emin, D.: Phys. Rev. B 40 (1989) 5649.

90A Aselage, T.L., Tallant, D.R., Gieske, J.H., Van Deusen, S.B., Tissot, R.G.: in: The Physics and Chemistry of Carbides, Nitrides and Borides; NATO ASI Series E: Applied Sciences Vol. 185, R. Freer ed., Kluwer Academic Publishers: Dordrecht, 1990, p. 97.

90W Werheit, H.: in: The Physics and Chemistry of Carbides, Nitrides and Borides; NATO ASI Series E: Applied Sciences Vol. 185, R. Freer ed., Kluwer Academic Publishers: Dordrecht, 1990, p. 705.

91P Papandreou, N., Zuppiroli, L.: in: Boron-Rich Solids, Proc. 10th Int. Symp. Boron, Borides and Rel. Compounds, Albuquerque, NM 1990 (AIP Conf. Proc. 231), D. Emin, T.L. Aselage, A.C. Switendick, B. Morosin, C.L. Beckel ed., American Institute of Physics: New York, 1991, p. 85.

91S1 Samara, G.A., Tardy, H.L., Venturini, E.L., Aselage, T.L., Emin, D.: in: Boron-Rich Solids, Proc. 10th Int. Symp. Boron, Borides and Rel. Compounds, Albuquerque, NM 1990 (AIP Conf. Proc. 231), D. Emin, T.L. Aselage, A.C. Switendick, B. Morosin, C.L. Beckel ed., American Institute of Physics: New York, 1991, p. 77.

91S2 Stein, H., Aselage, T.L., Emin, D.: in: Boron-Rich Solids, Proc. 10th Int. Symp. Boron, Borides and Rel. Compounds, Albuquerque, NM 1990 (AIP Conf. Proc. 231), D. Emin, T.L. Aselage, A.C. Switendick, B. Morosin, C.L. Beckel ed., American Institute of Physics: New York, 1991, p. 322.

91T1 Tallant, D.R., Aselage, T.L., Emin, D.: in: Boron-Rich Solids, Proc. 10th Int. Symp. Boron, Borides and Rel. Compounds, Albuquerque, NM 1990 (AIP Conf. Proc. 231), D. Emin, T.L. Aselage, A.C. Switendick, B. Morosin, C.L. Beckel ed., American Institute of Physics: New York, 1991, p. 301.

91T2 Tushishvili, M.Ch., Darsavelidze, G.Sh., Tsagareishvili, O.A., Bairamashvili, I.A., Jobava, J.Sh.: in: Boron-Rich Solids, Proc. 10th Int. Symp. Boron, Borides and Rel. Compounds, Albuquerque, NM 1990 (AIP Conf. Proc. 231), D. Emin, T.L. Aselage, A.C. Switendick, B. Morosin, C.L. Beckel ed., American Institute of Physics: New York, 1991, p. 582.

91T3 Tardy, H.L., Aselage, T.L., Emin, D.: in: Boron-Rich Solids, Proc. 10th Int. Symp. Boron, Borides and Rel. Compounds, Albuquerque, NM 1990 (AIP Conf. Proc. 231), D. Emin, T.L. Aselage, A.C. Switendick, B. Morosin, C.L. Beckel ed., American Institute of Physics: New York, 1991, p. 138.
91W1 Werheit, H., Haupt, H.: in: Boron-Rich Solids, Proc. 10th Int. Symp. Boron, Borides and Rel. Compounds, Albuquerque, NM 1990 (AIP Conf. Proc. 231), D. Emin, T.L. Aselage, A.C. Switendick, B. Morosin, C.L. Beckel ed., American Institute of Physics: New York, 1991, p. 355.
91W2 Werheit, H., Kuhlmann, U., Werheit, F.H., Krach, G.: in: Boron-Rich Solids, Proc. 10th Int. Symp. Boron, Borides and Rel. Compounds, Albuquerque, NM 1990 (AIP Conf. Proc. 231), D. Emin, T.L. Aselage, A.C. Switendick, B. Morosin, C.L. Beckel ed., American Institute of Physics: New York, 1991, p. 144.
91Z Zuppiroli, L., Papandreou, N., Kormann, R.: J. Appl. Phys. 70 (1991) 246.
92K1 Kuhlmann, U., Werheit, H., Schwetz, K.A.: J. Alloys Compounds 189 (1992) 249.
92K2 Kuhlmann, U., Werheit, H.: Solid State Commun. 83 (1992) 849.
92W Werheit, H., Laux, M., Kuhlmann, U., Telle, R.: Phys. Status Solidi (b) 172 (1992) K81.
93A Aselage, T.L., Emin, D., Samara, G.A., Tallant, D.R., van Deusen, S.B., Eatough, M.O., Tardy, H.L., Venturini, E.L.: Phys. Rev. B 48 (1993) 11759.
93E Emin, D.: Phys. Rev. B 48 (1993) 13691.
93K Kuhlmann, U., Werheit, H.: Phys. Status Solidi (b) 175 (1993) 85.
93S Samara, G.A., Tardy, H.L., Venturini, E.L., Aselage, T.L., Emin, D.: Phys. Rev. B 48 (1993) 1468.
93W Werheit, H., Kuhlmann, U.: Solid State Commun. 88 (1993) 21.
94A Aselage, T.L., Tallant, D.R., Emin, D., van Deusen, S.B., Yang, P.: Proc. 11th Int. Symp. Boron, Borides and Rel. Compounds, Tsukuba, Japan, August 22 - 26, 1993, Jpn. J. Appl. Phys. Series 10 (1994), p. 58.
94H Hori, A., Yamashita, H., Yamamoto, T., Tada, T., Kimura, K.: Proc. 11th Int. Symp. Boron, Borides and Rel. Compounds, Tsukuba, Japan, August 22 - 26, 1993, Jpn. J. Appl. Phys. Series 10 (1994), p. 100.
94K1 Kuhlmann, U.: Zusammenhänge zwischen den Phononenspektren borreicher Festkörper mit Ikosaederstruktur und ihren strukturellen und elektronischen Eigenschaften, Thesis, Gerhard-Mercator University, Duisburg, Germany, 1994.
94K2 Kuhlmann, U., Werheit, H.: J. Alloys Compounds 205 (1994) 87.
94K3 Kuhlmann, U., Werheit, H.: Proc. 11th Int. Symp. Boron, Borides and Rel. Compounds, Tsukuba, Japan, August 22 - 26, 1993, Jpn. J. Appl. Phys. Series 10 (1994), p. 94.
94K4 Kuhlmann, U., Werheit, H.: Proc. 11th Int. Symp. Boron, Borides and Rel. Compounds, Tsukuba, Japan, August 22 - 26, 1993, Jpn. J. Appl. Phys. Series 10 (1994), p. 84.
95L Li, Dong, Ching, W.Y.: Phys. Rev . B 52 (1995) 17073.
96W Werheit, H., Schmechel, R., Lundström, T., Tanaka, T., Ishizawa, Y.: (presented at the 12th Int. Symp. Boron, Borides and Rel. Compounds, Baden Austria, 1996, to be published separately).
97A Aselage, T., Tallant, D.R., Emin, D.: Phys. Rev. B 56 (1997) 3122.
97W Werheit, H., Janowitz, C., Schmechel, R., Tanaka, T., Ishizawa, Y.: J. Solid State Chem. 133 (1997) 132 (Proc. 12th Int. Symp. Boron, Borides and Rel. Compounds, Baden, Austria, Aug. 25 - 30, 1996).
98S1 Schmechel, R.: Thesis, Gerhard-Mercator University Duisburg, Germany, 1998.
98S2 Schmechel, R., Werheit, H.: J. Mater. Process. Manufact. Sci. 6 (1998) 329 (Proc. NATO ASI on Material Science of Carbides, Nitrides and Borides, St. Petersburg, Russia, Aug. 12-22, 1998).
99S1 Shirai, K., Katayama-Yoshida, H.: J. Solid State Chem. (2000) (Proc. 13th Int. Symp. Boron, Borides and Rel. Compounds, Dinard, France, Sept. 1999).
99S2 Schmechel, R., Werheit, H.: J. Phys.: Condens. Matter 11 (1999) 6803.
99W1 Werheit, H., Schmechel, R., Kuhlmann, U., Kampen, T.U., Mönch, W., Rau, A.: J. Alloys Compounds 291 (1999) 28.
99W2 Werheit, H., Au, T., Schmechel, R., Shalamberidze, S.O., Kalandanze, G.I., Eristavi, A.M.: J. Solid State Chem. (2000) (Proc. 13th Int. Symp. Boron, Borides and Rel. Compounds, Dinard, France, Sept. 1999).
99W3 Werheit, H., Schmechel, R., Kuhlmann, U., Kampen, T.U., Mönch, W., Rau, A.: in: 13th Int. Symp. Boron, Borides and Rel. Compounds, Dinard, France, Sept. 1999 (see also 99W 3).

Fig. 1.

Boron carbide ($B_{13}C_2$). Calculated optical properties. vs. photon energy. **(a)** Optical conductivity, **(b)** dielectric function, **(c)** energy-loss function [95L].

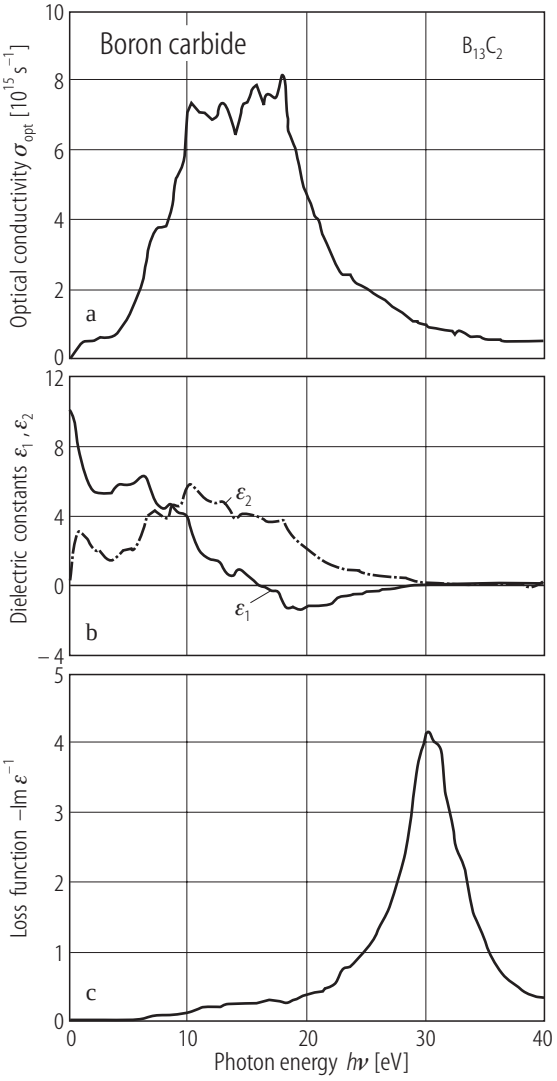

Fig. 2.

Boron carbide ($B_{11}C$ (CBC)). Calculated optical properties vs. photon energy. **(a)** Optical conductivity, **(b)** dielectric function, **(c)** energy-loss function [95L].

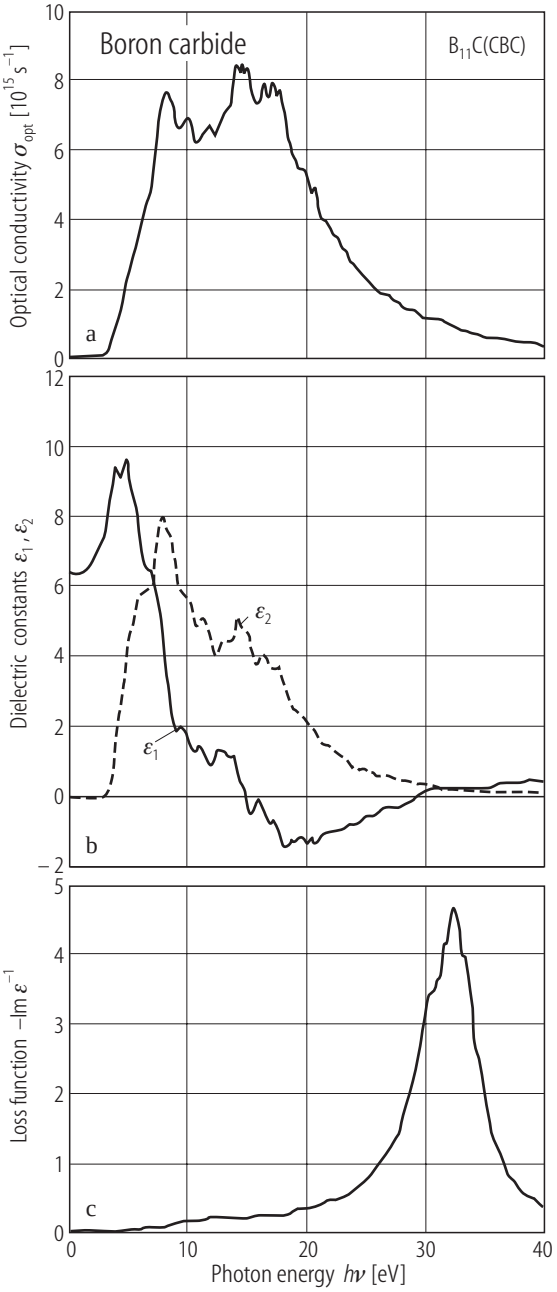

Fig. 3.

Boron carbide. Real part of the dielectric function ε_1 and tanδ vs. temperature. **(a)** $B_{4.5}C$; **(b)** B_9C. Insert: frequency dependence of ε_1 [93S]

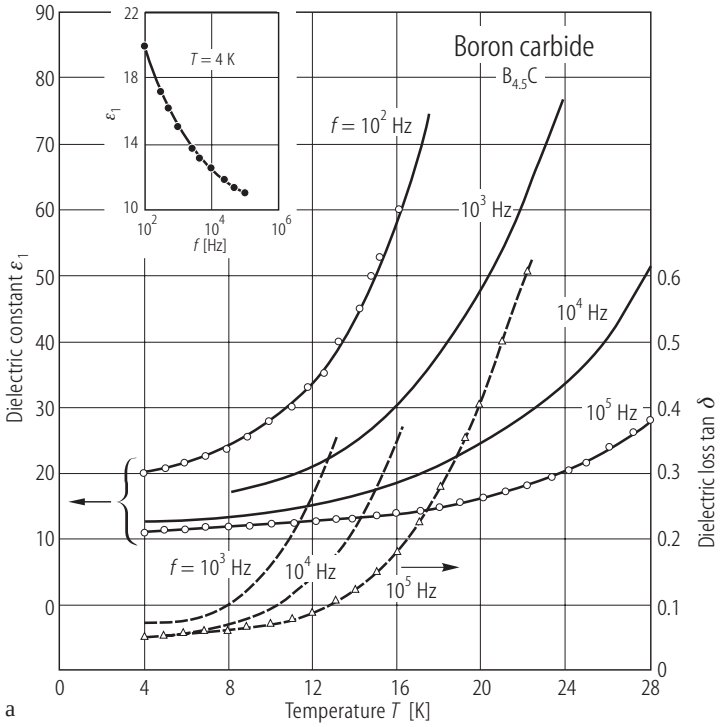

a

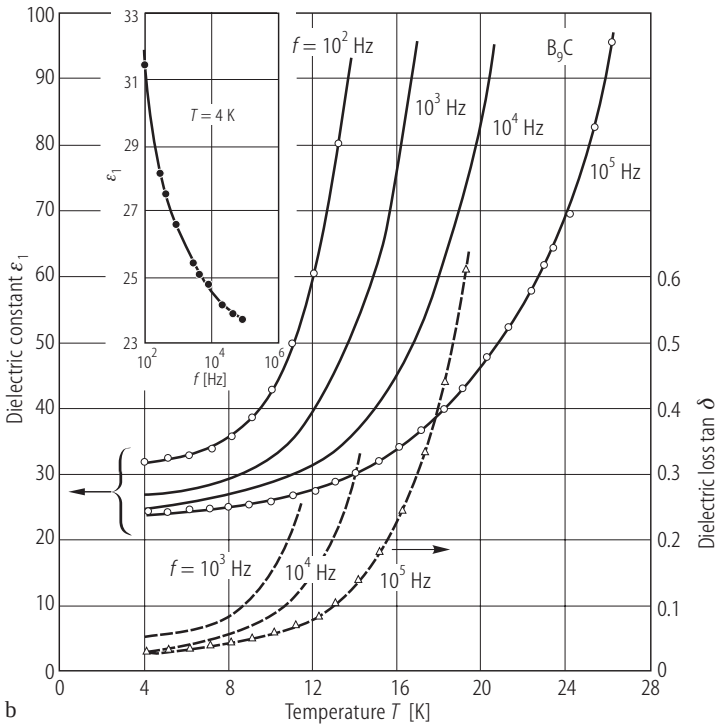

b

Fig. 4.

Boron carbide. Real part of the dielectric function ε_1 vs. frequency for B_xC at 4 K (x = 4.33; x = 4.5, x = 5.5, x = 9.0) [93S].

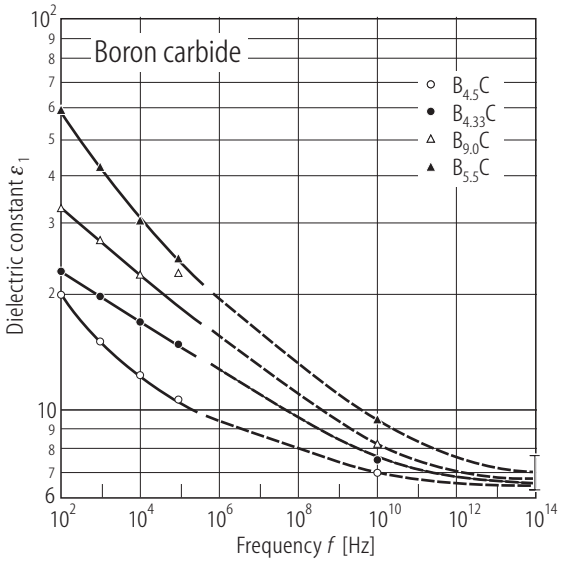

Fig. 5.

Boron carbide. Real part of the dielectric function ε_1 vs. frequency for. **(a)** $B_{4.3}C$ (T = 8, 15, 22, 36, 46 and 60 K), **(b)** $B_{13}C_2$ (T = 4, 10 and 40 K) [91Z, 91P, 91S1].

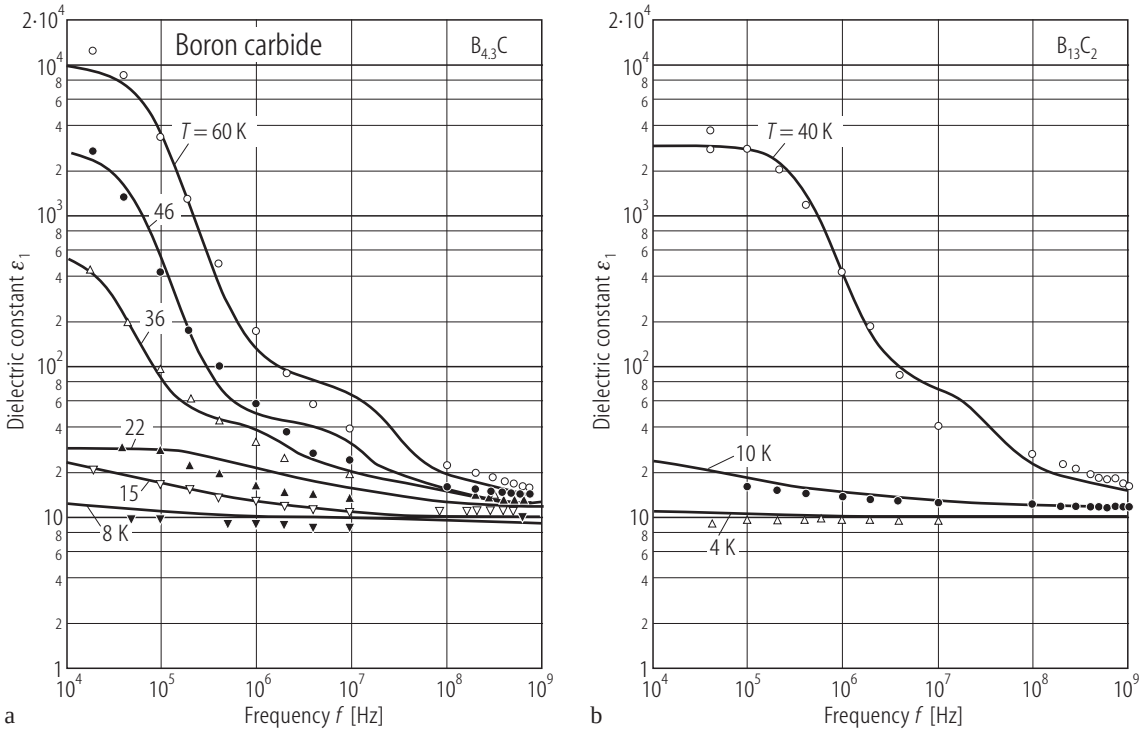

Fig. 6.

Boron carbide (B_4C. Dielectric function at 9 GHz vs. temperature [91Z].

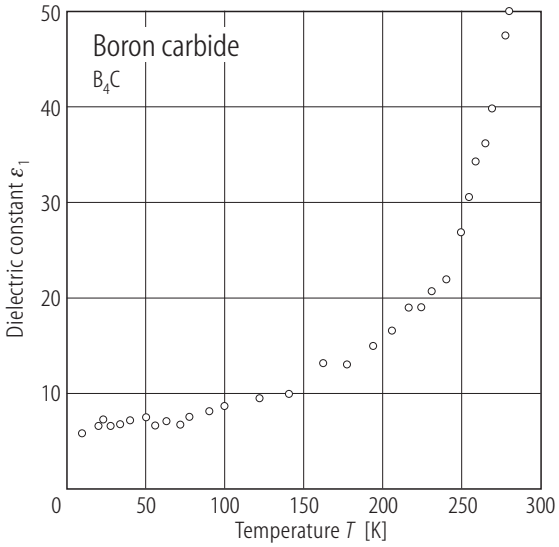

Fig. 7.

Boron carbide ($B_{4.3}C$). Real part of the dielectric function vs. frequency. Experimental results: (——) optical [98S1, 98S2]; symbols [91Z]; (-----) impedance analysis [98S1, 98S2]. Model calculations [98S1, 98S2] based on different theories: (–···–···–···) extended Drude model [85M]; (·····) hopping model; (-··-··-··-) [73B], potential fluctuations [84P]; (-·-·-·-·-) random free energy barrier model [88D].

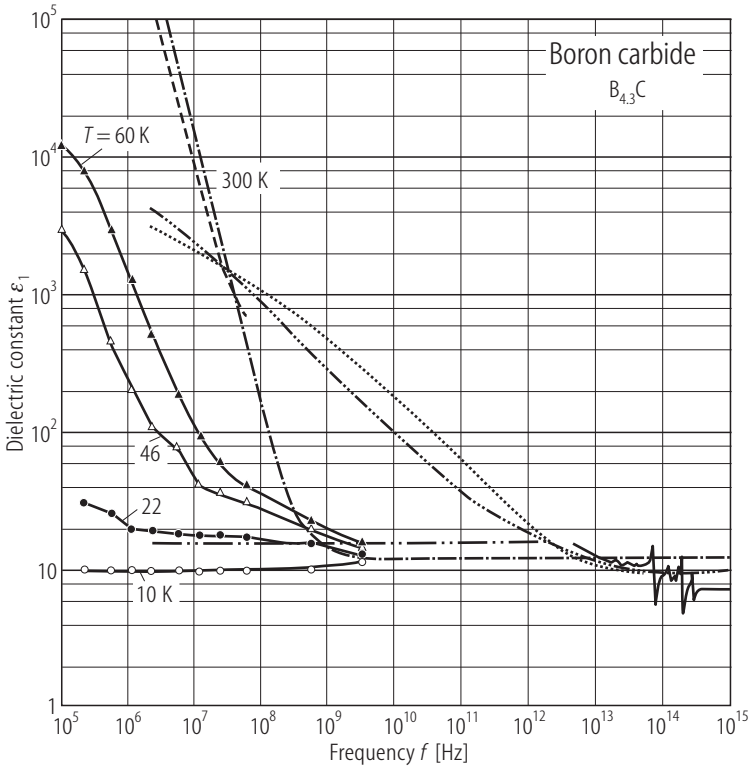

Fig. 8.

Boron carbide ($B_{6.3}C$). Optical conductivity and real part of the dielectric function vs. wavenumber for 90, 300 and 450 K. Experimental, full structured line [98S1, 99S2]; fits (phonons ignored): (——) extended Drude model, (-----) hopping model, (–·–·–·–) potential fluctuations, (·····) hopping + Drude, (–··–··–) deep level absorption according to [65L]. For references of the transport models, see Fig. 7. ·

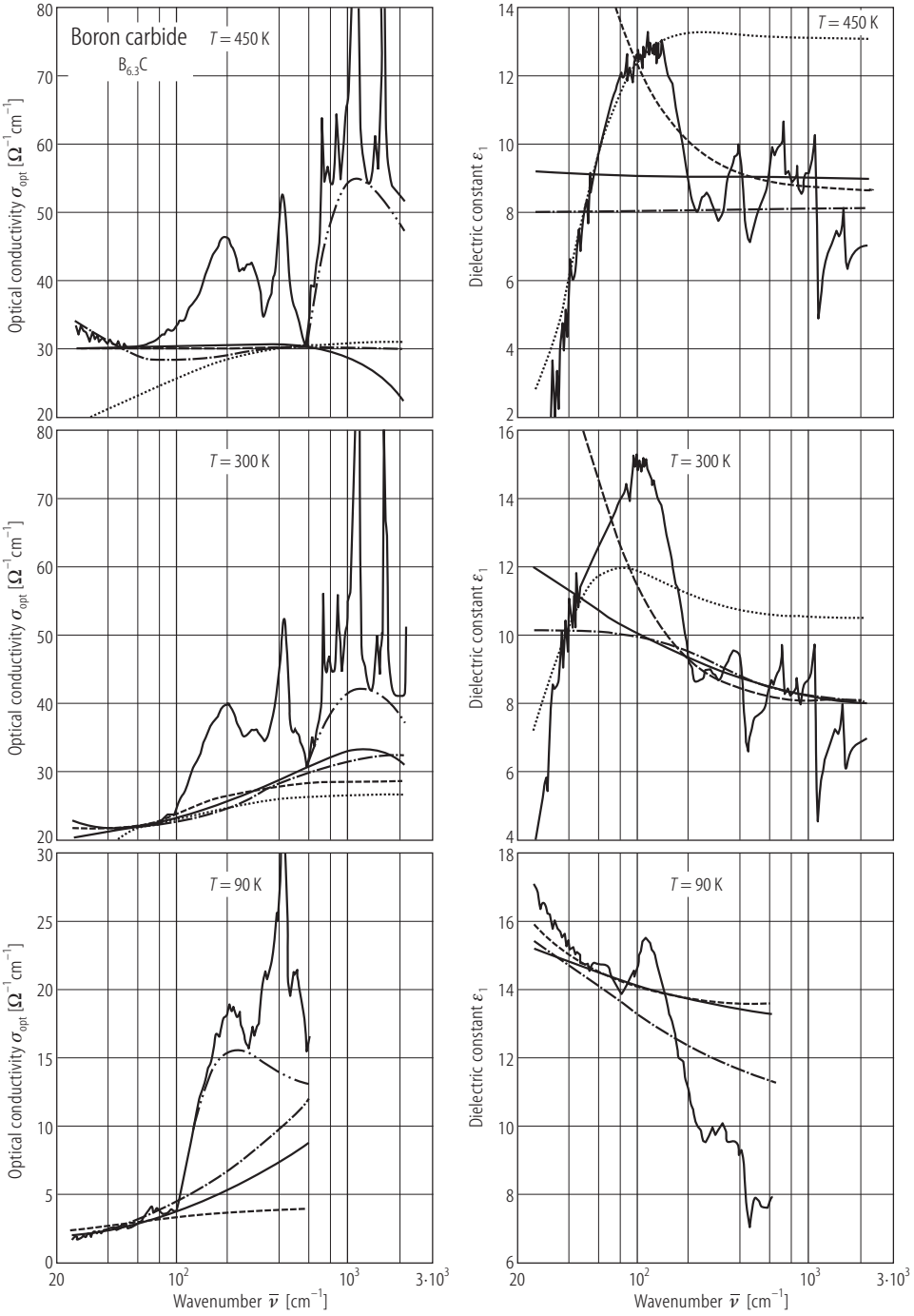

Fig. 9.

Boron carbide. **(a)** Real and **(b)** imaginary part of the dielectric function vs. photon energy for $B_{4.23}C$, $^{10}B_{4.3}C$, $B_{4.51}C$, $B_{6.28}C$, $B_{8.52}C$, $B_{10.37}C$ at T = 4 K [97W].

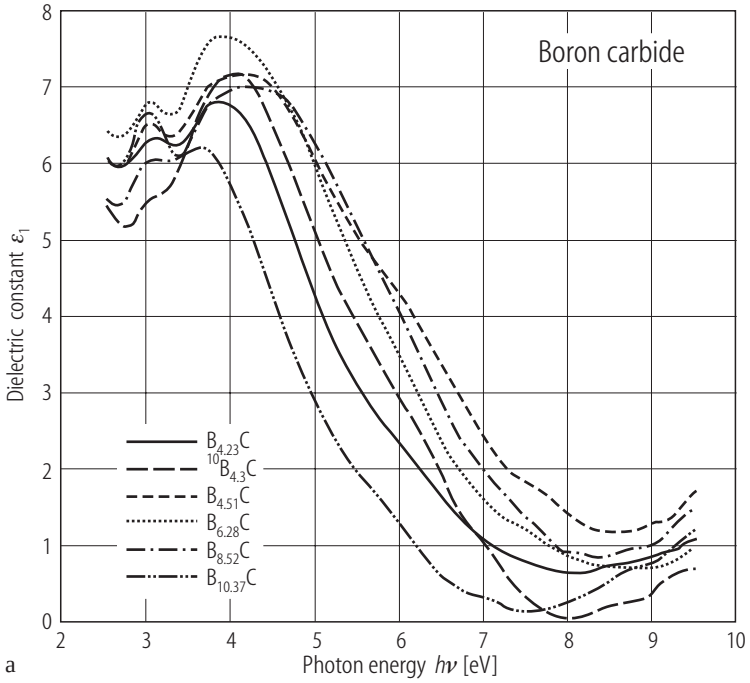

a

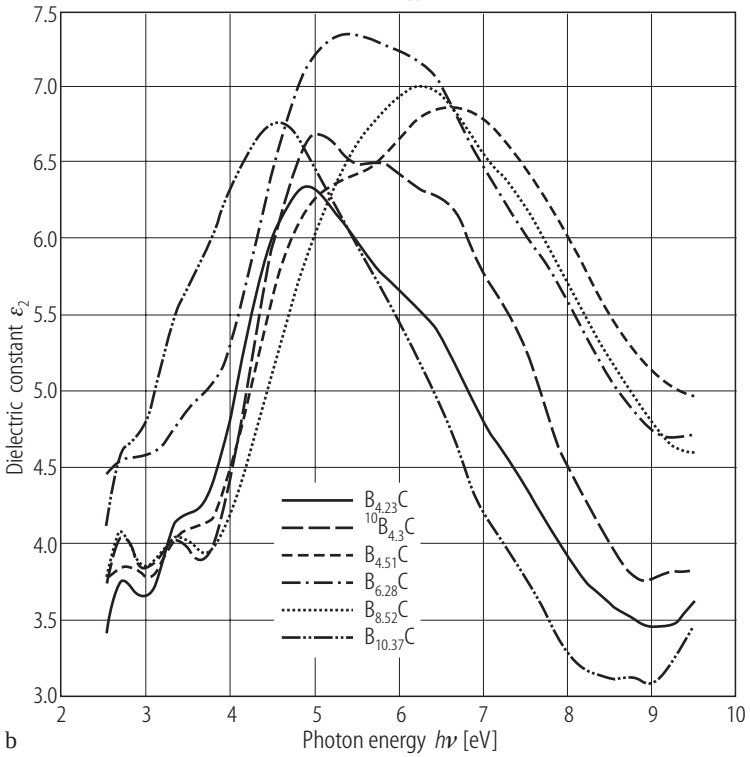

b

Fig. 10.

Boron carbide (~$B_{4.3}C$). Absorption coefficient of different boron carbide specimens vs. photon energy in the spectral range of the absorption edge. The sharp absorption bands between 0.3 and 0.45 eV are caused by the C-H vibrations of the organic glue, by which the specimens were adhered to the quartz support. F 1500, prepared by MPI Stuttgart from extremely fine powder (H.C. Starck), HIP (2100 °C, 30 MPa, 30 min, vacuum) traces of WC; HPB4C, commercial boron carbide, axial hot-pressed (Elektroschmelzwerk Kempten, ESK); HDB4C, commercial boron carbide, pressureless sintered, then hot isostatically compressed (Elektro-schmelzwerk Kempten, ESK); BCSIN, self-supporting sample of commercial boron carbide, axial hot pressed with 6 MPa (HC Starck) [92W]. Because of the difficulty to determine the sample thickness, the uncertainty of the absolute values may be up to 25 %. (HIP: hot isostatically pressed).

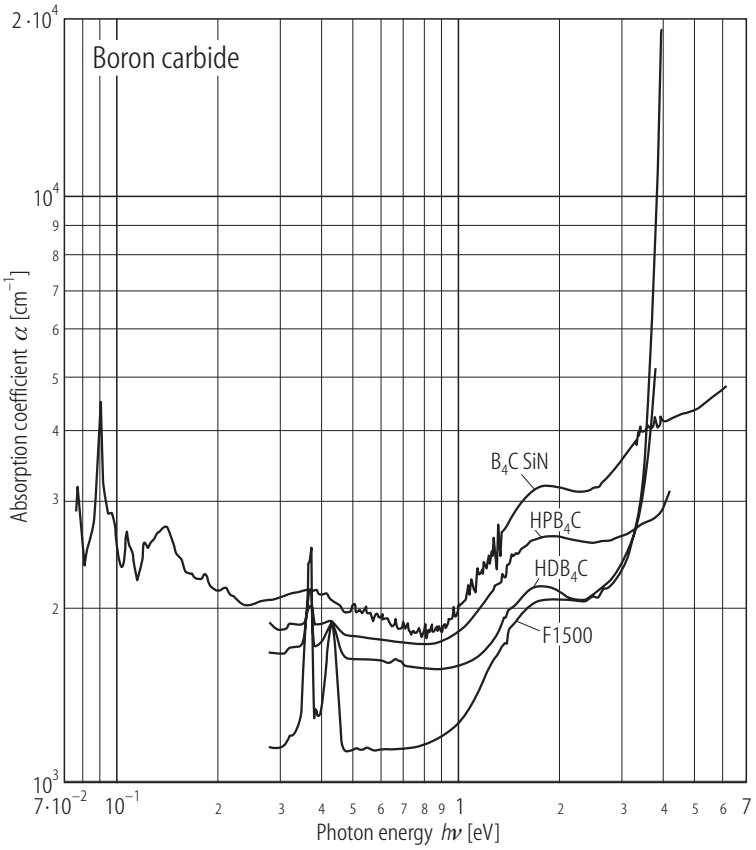

Fig. 11.

Boron carbide (~$B_{4.3}C$). Isotherms of the absorption coefficient of F 1500 (see Fig. 10) between 80 and 590 K [92W].

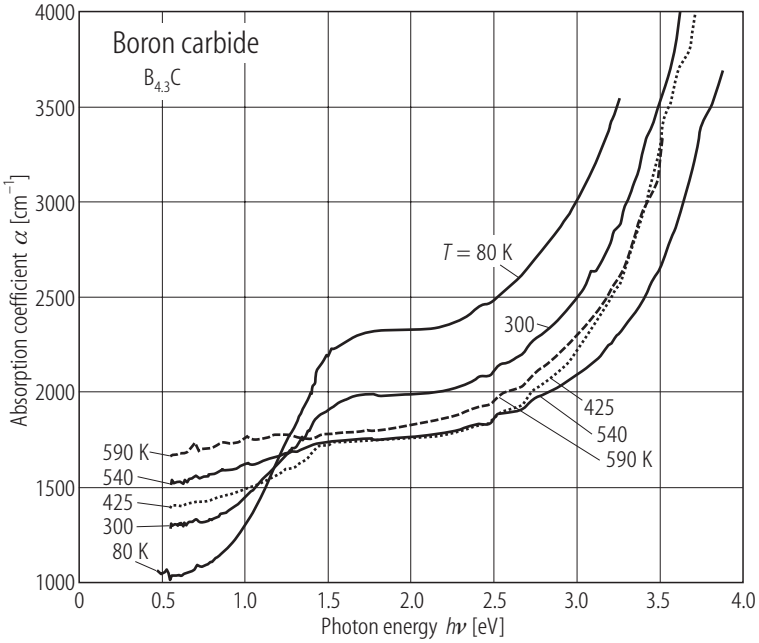

Fig. 12.

Boron carbide (B_4C). Reflectance vs. photon energy (β-rhombohedral boron for comparison) [94H].

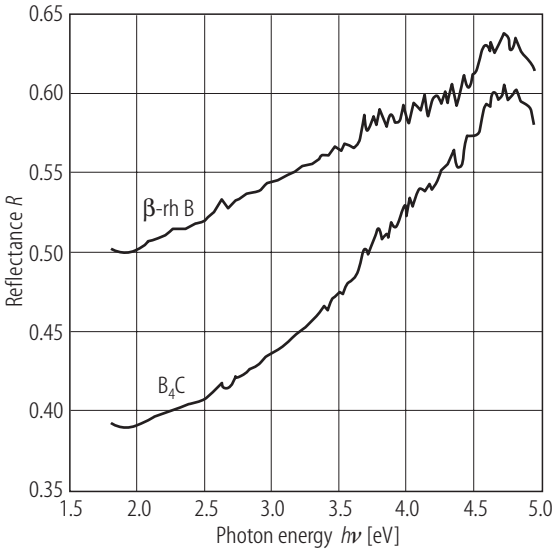

Fig. 13.

Boron carbide. Structure-modulated reflectivity spectra $\Delta R/R$ and their first derivatives obtained on boron carbide ($^{10}B_{4.3}C$, $^{nat}B_{4.3}C$, $^{nat}B_{4.52}C$,) vs. photon energy [96W].

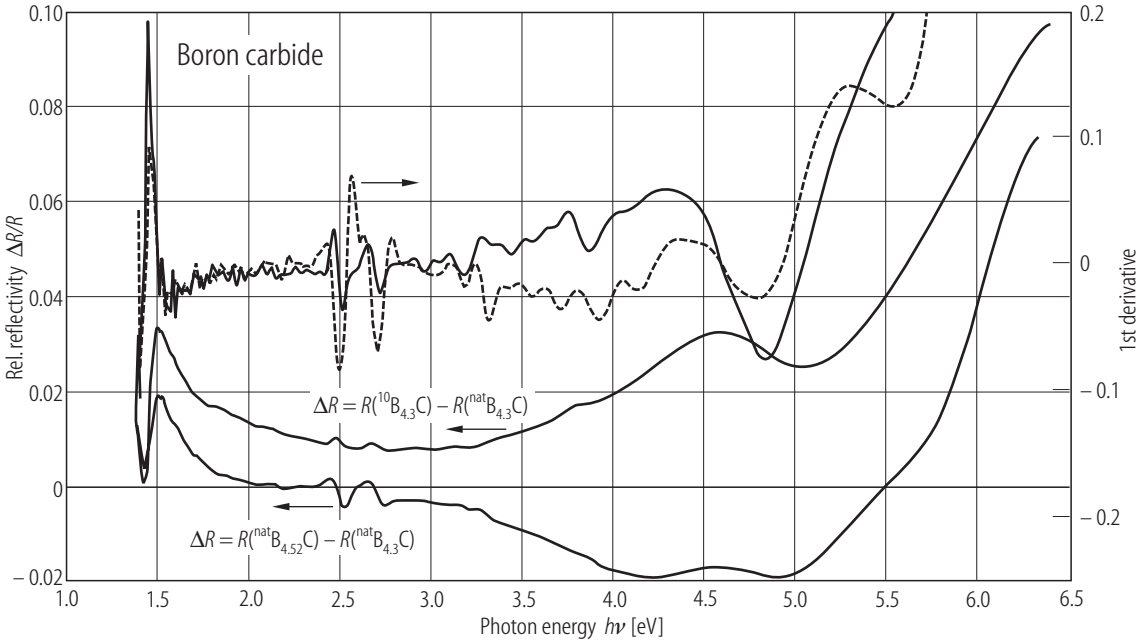

Fig. 14.

Boron carbide. Structure-modulated reflectivity spectra $\Delta R/R$ (related to $B_{4.23}C$ each) vs. photon energy. The spectra are normalized in such a way that they were related to a straight line determined by the minima in the spectra at about 1.4 and 4.5 eV each. By this procedure the influence of light scattering on the specific spectra was roughly eliminated [96W].

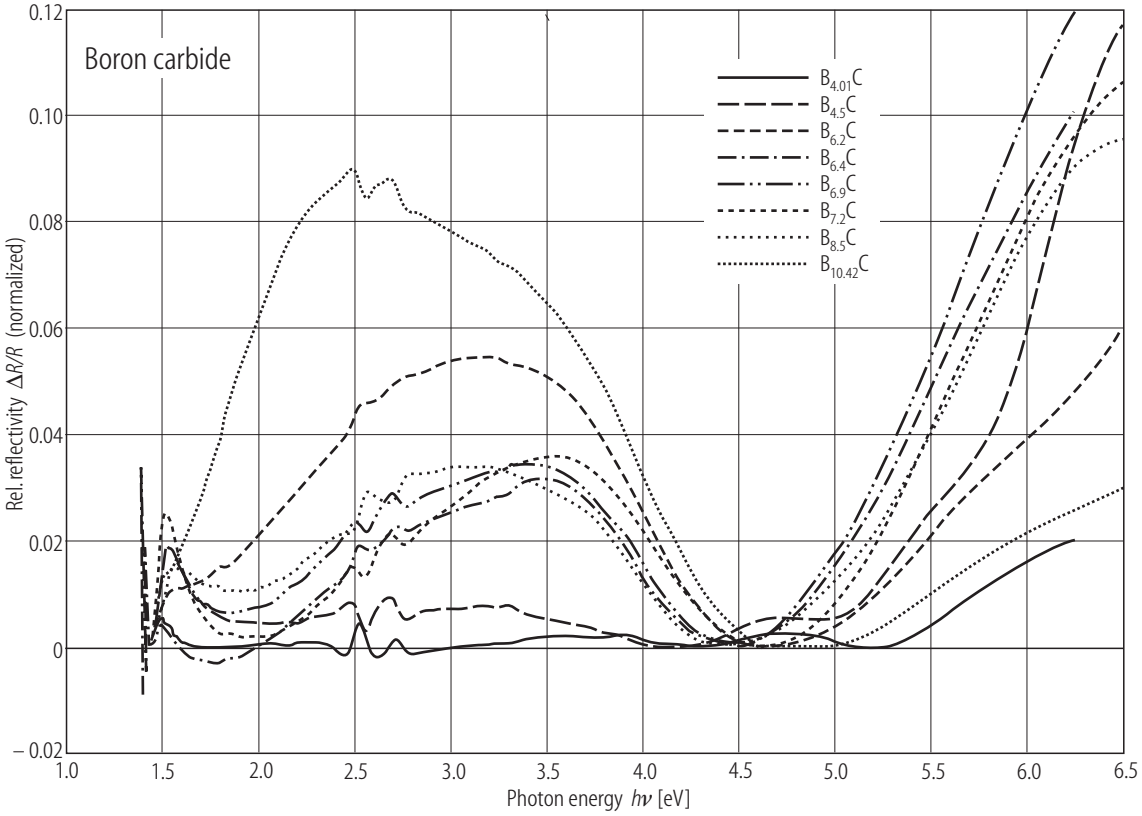

Fig. 15.

Boron carbide. FIR reflecticvity vs. wavenumber; **(a)** $B_{4.3}C$, **(b)** $B_{6.3}C$, **(c)** $B_{10.37}C$ [98S1, 99S2].

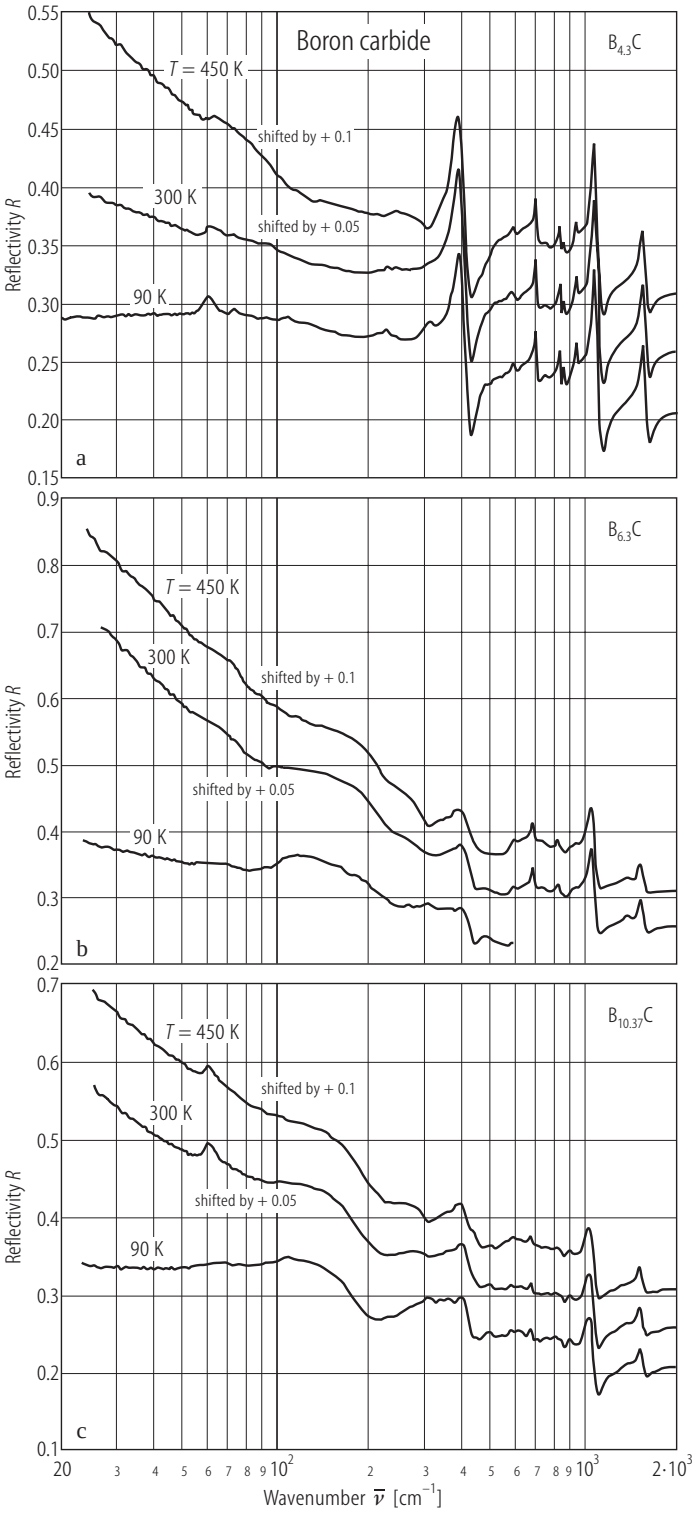

Fig. 16.

Boron carbide. Spectra of the IR active phonons of $B_{4.3}C$, $B_{6.3}C$, $B_{7.91}C$, $B_{8.52}C$ and $B_{10.37}C$ at T = 160 K [92K1, 92K2, 94K1, 94K4].

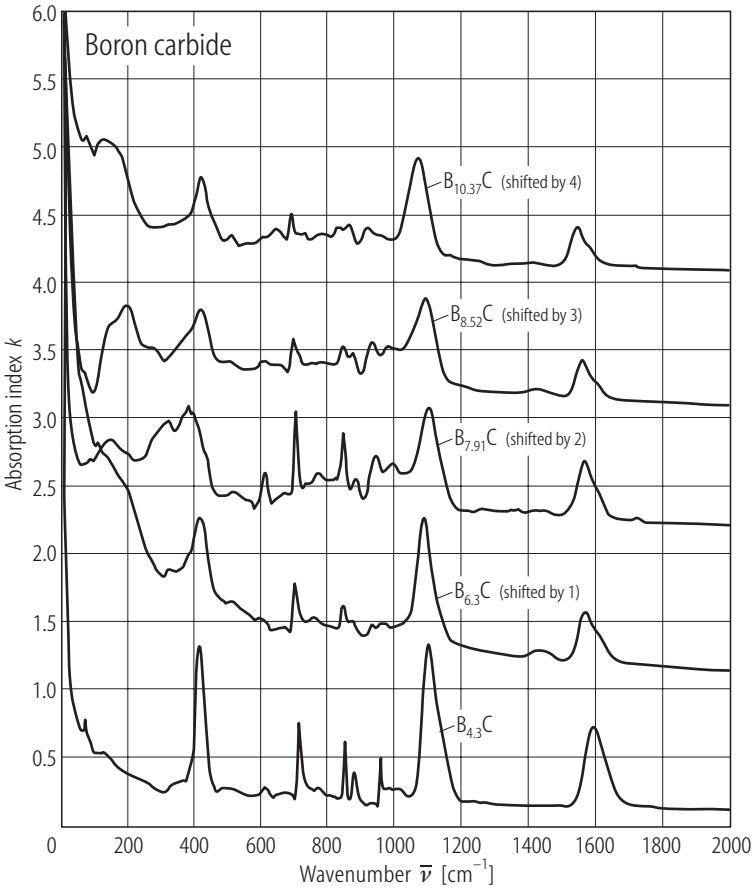

Fig. 17.

Boron carbide ($B_{4.3}C$). Optical spectra of the IR active phonons; **(a)** reflectivity, **(b)** absorption index vs. wavenumber [92K1, 92K2, 94K1].

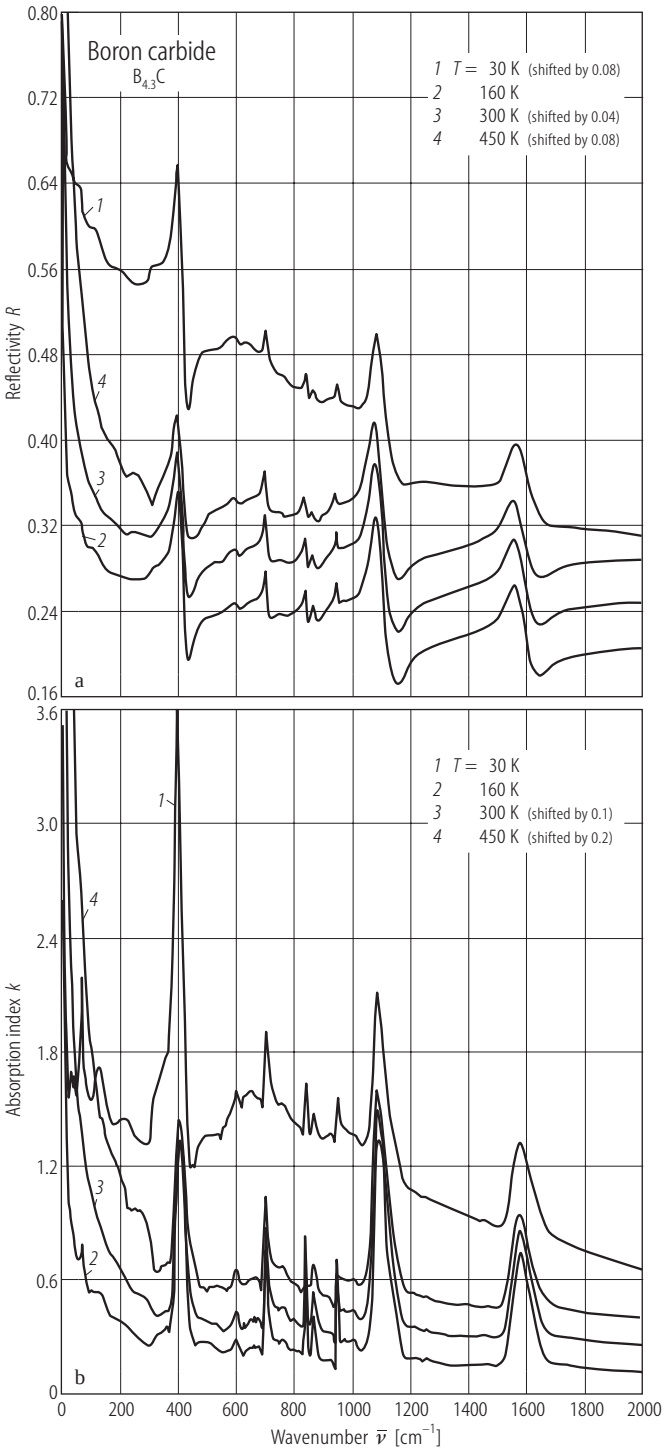

Fig. 18.

Boron carbide ($B_{\sim 4.3}C$). Spectra of the IR active phonons. **(a)** Reflectivity, **(b)** absorption index vs. wavenumber for $B_{4.3}C$ with natural isotope distribution (unpolarized radiation), $B_{4.3}C$ with natural isotope distribution ($E \perp c$), isotope enriched $B_{4.3}C$ (92% ^{10}B) [92K1, 92K2, 94K1].

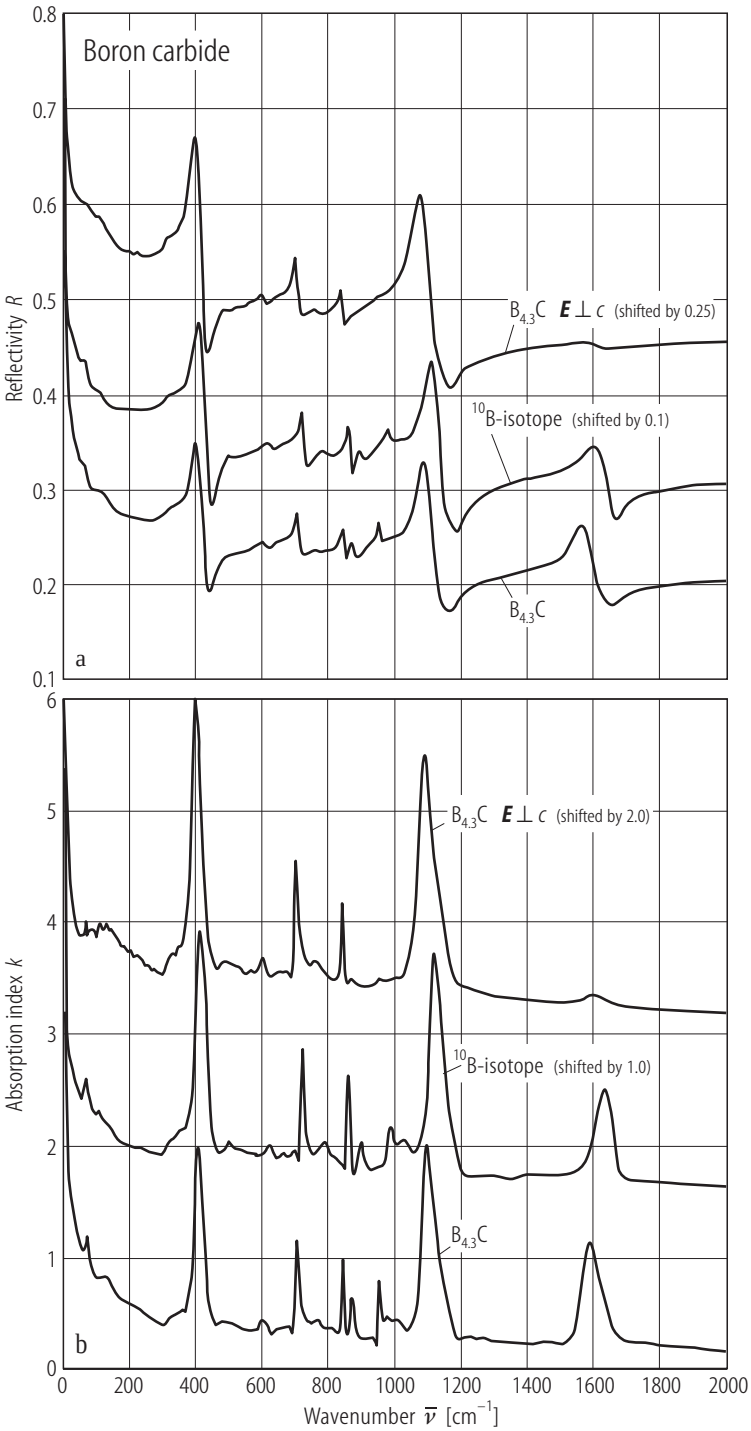

Fig. 19.

Boron carbide ($B_{\sim 4.3}C$). Spectra of the IR-active phonons of isotope-enriched boron carbide: $^{10}B_{4.3}C$, $^{11}B_{4.3}C$, $^{10}B_{4.3}{}^{13}C$; enrichment: 98.4 at.% ^{10}B, 99.4(2) at.% ^{11}B and 80.1(2) at.% ^{13}C, respectively. Impurities are Fe (0.6 mass %) and Mg, Si, Al, Ca, Cu (in total 1.3 wt.%). **(a)** Reflectivity; **(b)** absorption index [99W2]. For the corresponding spectra of $B_{6.5}C$ and $B_{10}C$ see ref.

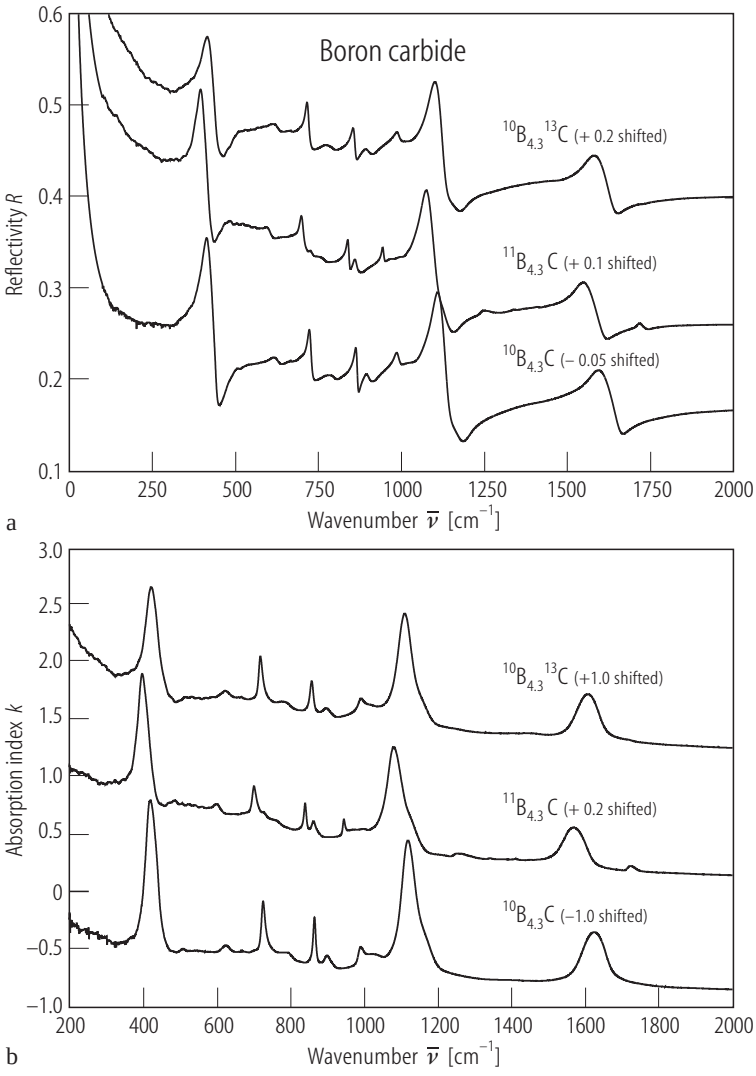

Fig. 20.

Boron carbide. Absorption spectra of the stretching mode of the three-atom chain for different chemical compositions and isotope enrichments. **(a)** Experimental results; **(b)** calculated relative probability distributions of the resonance frequencies for different possible combinations of chain atoms (top) $B_{4.3}C$ with natural isotope distribution, (bottom) $^{10}B_{4.3}C$ (^{10}B, 92% enriched) [92K1, 92K2, 94K1].

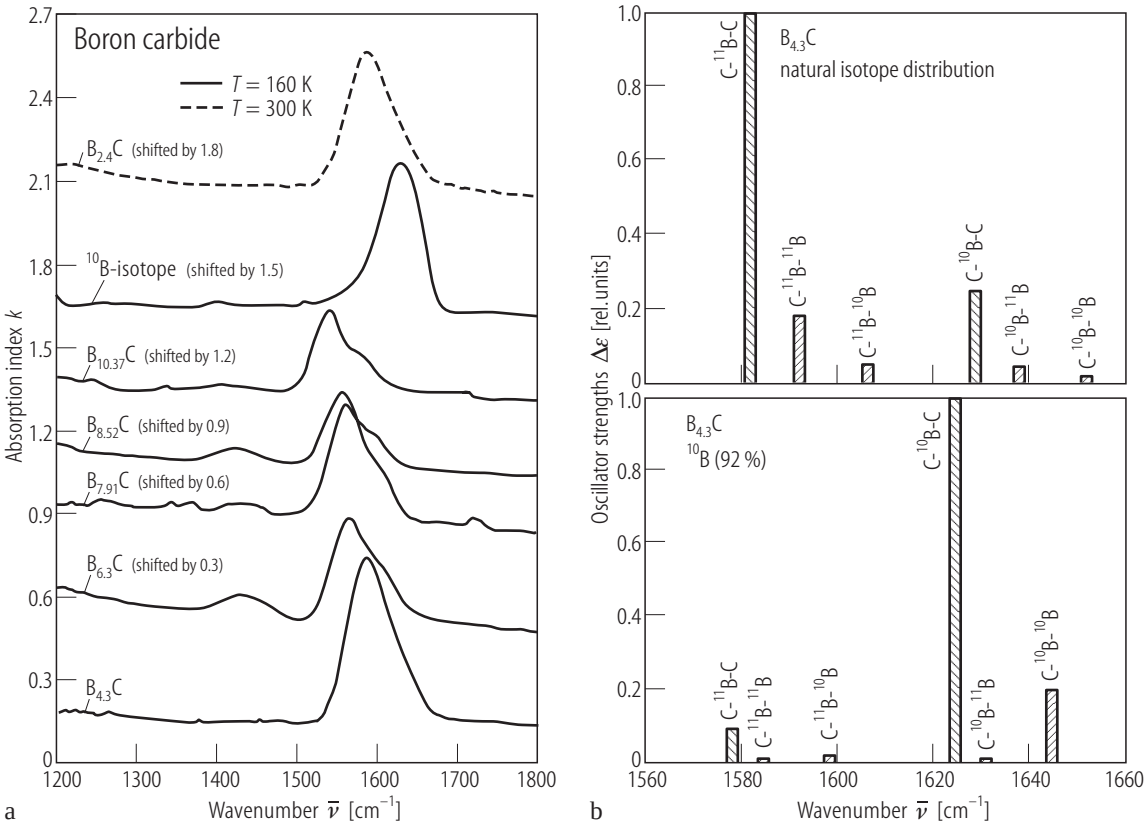

Fig. 21.

Boron carbide (~$B_{4.3}C$). Stokes and low-energy anti-Stokes FT-Raman spectrum of polycrystalline $B_{4.3}C$; resolution 2 cm^{-1}. Dashed line, calculated anti-Stokes spectrum based on the measured Stokes spectrum and a sample temperature of 330 K [93K, 94K1, 94K2, 94K3]. Bottom: conventionally measured Raman spectrum [88T, 89T, 91T1, 90A].

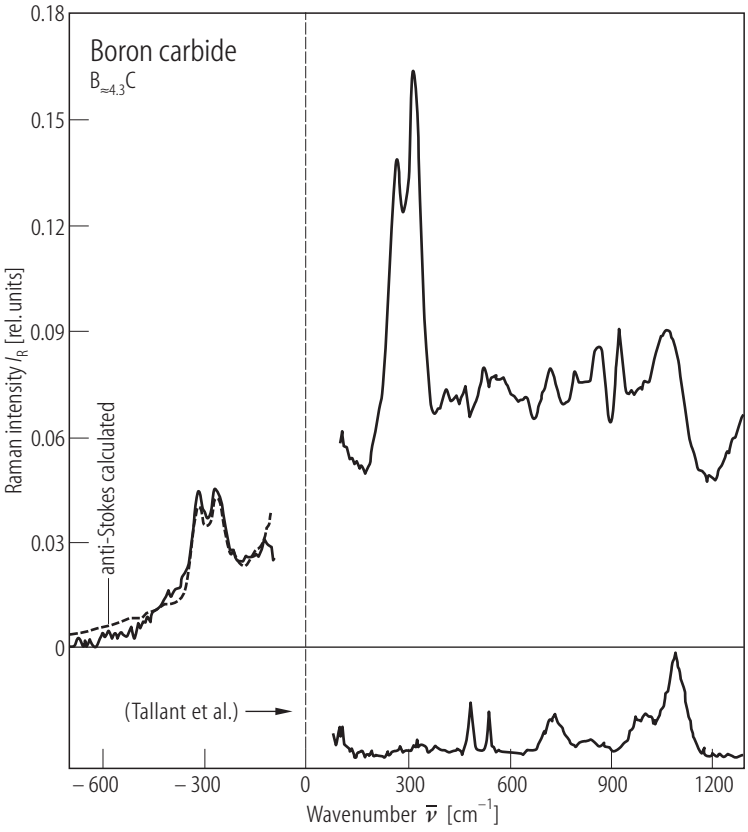

Fig. 22.

Boron carbide. FT-Raman spectra (resolution 2 cm^{-1})vs. Raman shift. $^{10}B_{4.3}C$ (92% ^{10}B enriched, unpolarized) and $^{nat}B_{4.3}C$ (unpolarized and polarized $c(x_i x_j)c$, i.e. all directions perpendicular to the crystallographic c axis) [94K1].

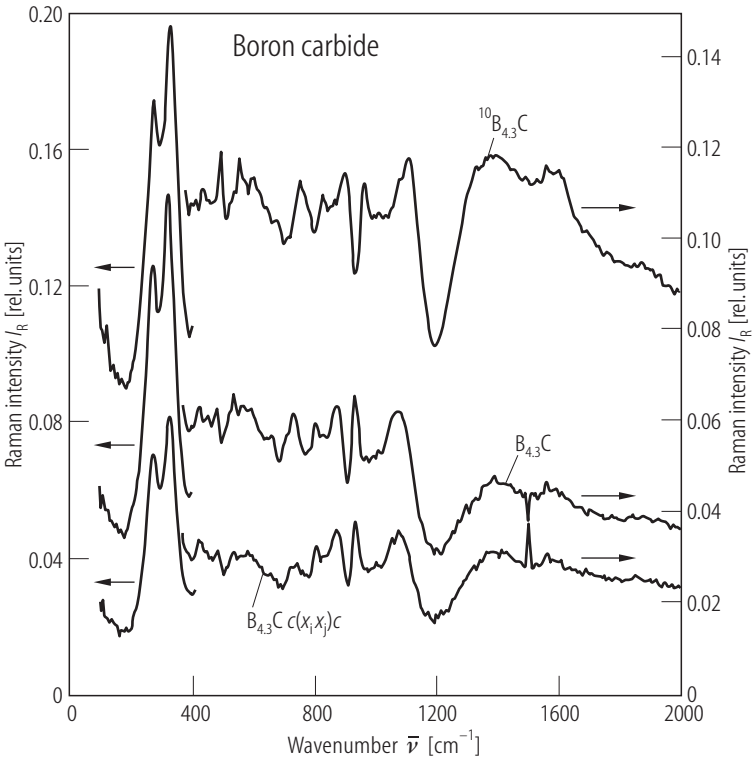

Fig. 23.

Boron carbide. FT-Raman spectra (resolution 2 cm^{-1}) vs. Raman shift for $B_{4.3}C$, $B_{6.3}C$, $B_{7.91}C$, $B_{8.52}C$, $B_{10.37}C$ [94K1, 94K2, 94K3].

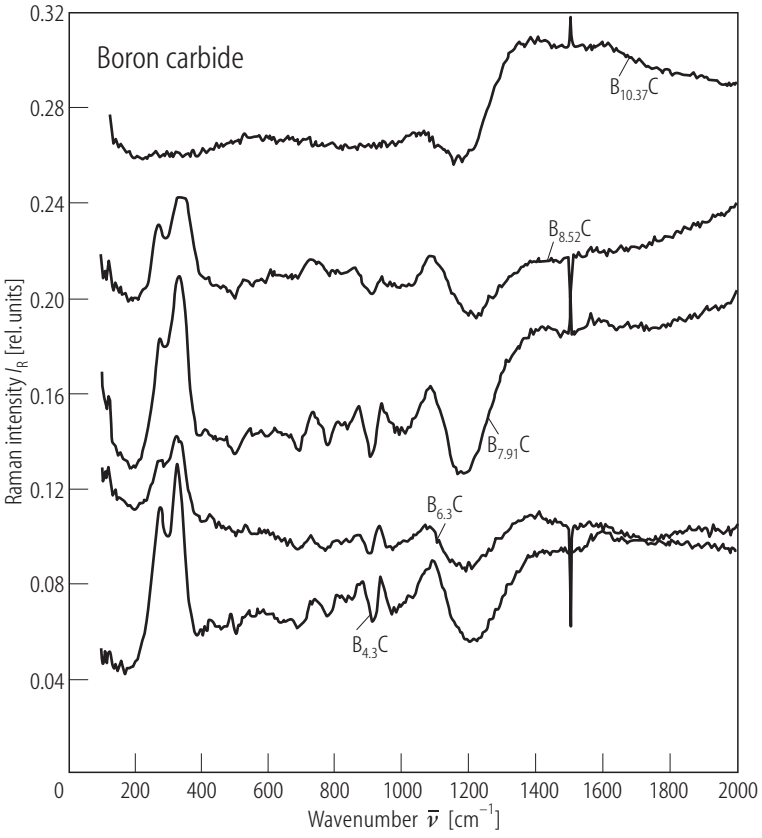

Fig. 24.

Boron carbide. (unknown composition; approximately $B_{12}C_3$, polycrystalline samples). Absorption coefficient vs. wavelength [71W, 74W].

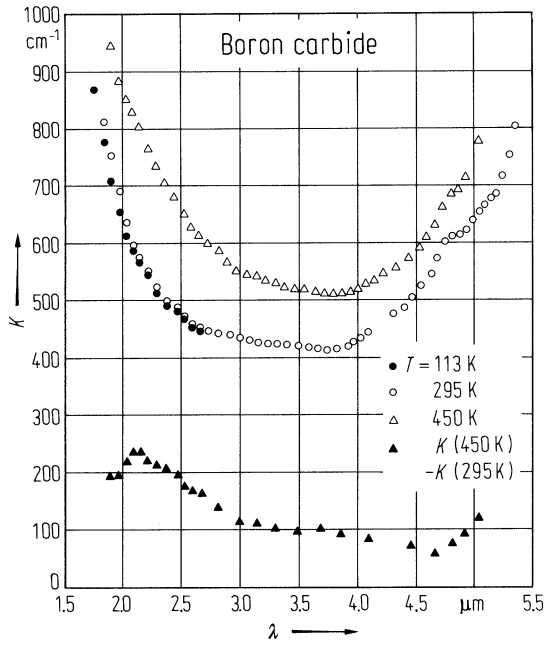

Fig. 25.

Boron carbide (unknown composition; approximately $B_{12}C_3$) Photoabsorption at 113 K. Optical excitation spectrum of optically excited and trapped electrons into the conduction band, absorption cross section *q*, times medium concentration of absorption centers per unit area, *N*, vs. photon energy [71W, 74W].

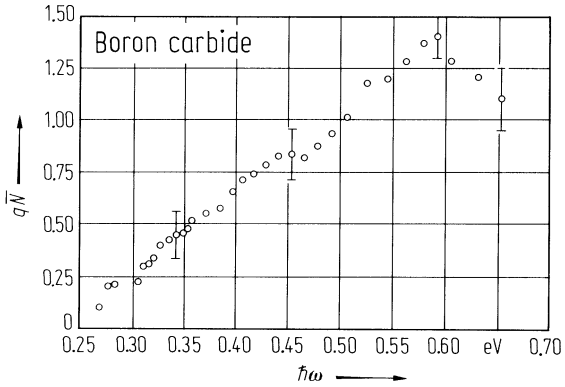

Fig. 26.

Boron carbide. (unknown composition; approximately $B_{12}C_3$) Concentration of unoccupied traps at 113 K; dependence on the time of photo-excitation, measured by optical absorption at λ =3.25 μm [71W].

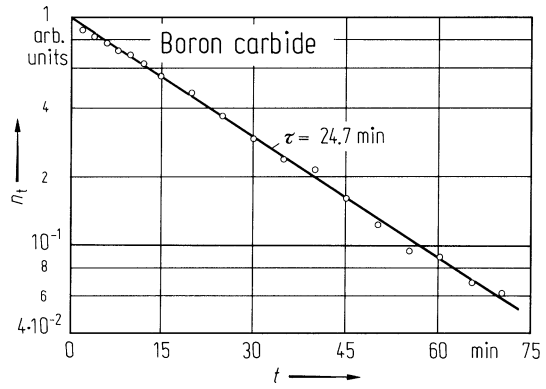

Fig. 27.

Boron carbide. (unknown composition; approximately $B_{12}C_3$) IR reflectivity vs. wavenumber. The sample dependent increase of R to wavenumbers < 350 cm^{-1} is attributed to the plasma resonance of free carriers [79B].

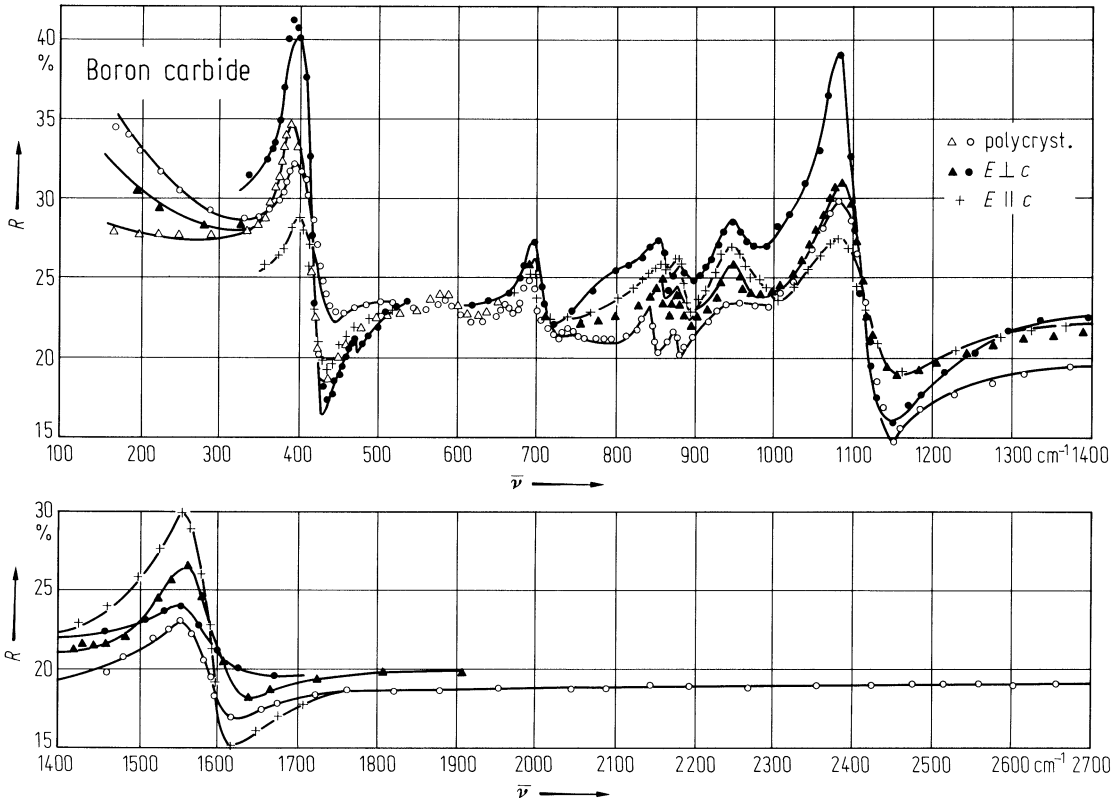

Fig. 28.

Boron carbide. Relative difference of the reflectivity spectra of boron carbide with various carbon contents obtained by sample-modulation spectroscopy vs. photon energy. —— : $R_{sample1} - R_{sample4}$; ----: $R_{sample4} - R_{sample5}$; ⋯:$R_{sample4} - R_{sample6}$. The zero point is arbitrarily chosen, hence a relatively higher reflectivity of the more boron-rich samples is indicated by more positive values, a relatively higher reflectivity of more carbon-rich samples by more negative values [79W].

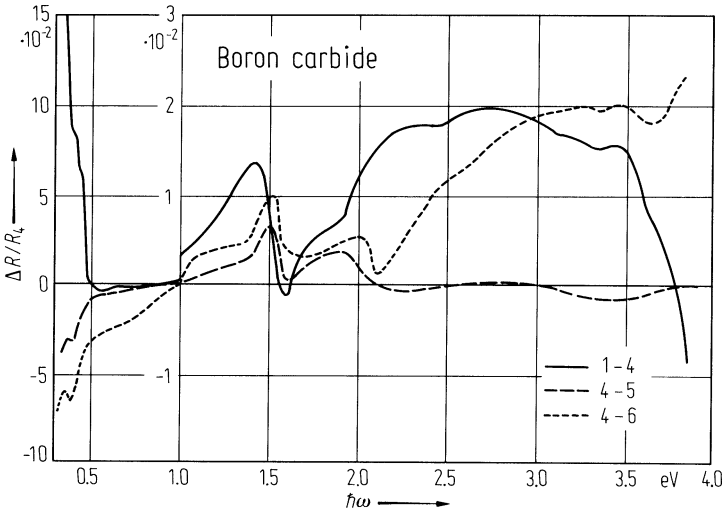

Fig. 29.

Boron carbide. Light-induced change of the differential reflectivity of two samples with different C contents ($(R_1–R_4)_{photo}/R_4$) vs. photon energy [79W]. R_1: $R_{sample1}$, R_4: $R_{sample4}$.

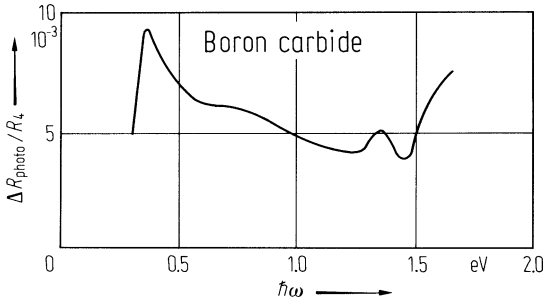

Fig. 30.

Boron carbide. a) Relative shift of the resonance wavenumber of IR-active phonons at RT (1080 cm^{-1} phonon: split icosahedral mode; 1580 cm^{-1} phonon: vibration of the C–B–C chain) vs. carbon content [82W] (cp. also [81E, 81B2]). b) Oscillor strength of the phonons vs. carbon content [82W].